Influence of silicon on the oxidation of iron-based amorphous alloys

W. D. ROOS, G. N. VAN WYK
Department of Physics, University of the Orange Free State, PO Box 339, ZA-9300 Bloemfontein, Republic of South Africa

The room-temperature oxidation behaviour of three different iron-based amorphous alloys, $Fe_{78}B_{13}Si_9$, $Fe_{79}B_{16}Si_5$ and $Fe_{81}B_{13.5}Si_{3.5}C_2$, was studied by Auger electron spectroscopy and X-ray photoelectron spectroscopy. The oxides which formed were characterized and the influence of alloy composition on the oxidation rate was determined. The presence of chromium in the 5 at% Si specimen increased the oxidation rate of the boron in the alloy. Oxidation-induced segregation of boron led to boron enrichment in the oxide layer. No positive influence of silicon content on the oxidation behaviour could be detected.

1. Introduction

In addition to the interesting magnetic, electrical and mechanical properties of amorphous alloys, it is well known that these alloys also possess high corrosion resistance when compared to crystalline alloys [1]. Many investigations have aimed to clarify whether the oxidation properties result from the amorphous structure or from the presence of elements such as phosphorous, boron, chromium and silicon [2–6].

Fusy and Pareja [7] studied the surface oxidation of two iron-based amorphous and crystallized alloys. They concluded that the state of crystallinity has no effect on the rate of oxygen uptake on the $Fe_{15}P_{15}C_{10}$ alloy but that the superficial phosphorus content was the determining factor. In the case of the $Fe_{85}B_{15}$ alloy the change in oxygen uptake on the amorphous and crystalline alloys and on pure iron was of the same rate.

Karve *et al.* [3] made a comparative study of surface oxidation behaviour of an amorphous and crystallized alloy containing chromium and phosphorus. They found that the oxygen uptake on the crystallized sample was much higher than on the amorphous sample, and concluded that the constant ratio between chromium and phosphorus in the oxide film for both samples (amorphous and crystallized) indicated the importance of the amorphous state for high oxidation resistance, in addition to the presence of chromium and phosphorus.

Myhra *et al.* [2] investigated the early stages of oxidation at room temperature of amorphous $Fe_{70}Cr_{15}B_{15}$ and $Fe_{85}B_{15}$. It was shown that the presence of chromium promoted the initial reactivity of boron and iron towards oxygen by two orders of magnitude compared to the $Fe_{85}B_{15}$ alloy.

In this study the oxides formed at room temperature of three similar iron-based amorphous alloys containing different concentrations of silicon were characterized. The alloys also contained boron and carbon in varying quantities. The initial aim of the study was to determine the influence of silicon content on the oxidation behaviour, but during the analysis it was found that one of the alloys contained chromium (< 4 at %) as an impurity. Not only had this to be taken into account in the analysis of the results, but it also offered the opportunity of studying the influence of the presence of chromium (in addition to silicon) in one of the specimens. The analysis was restricted to room temperature, firstly to keep the alloys amorphous and secondly to prevent silicon enrichment of the surface due to segregation at higher temperatures [8].

2. Experimental procedure

Three iron-based amorphous alloys were investigated. The compositions were specified by the manufacturers as $Fe_{78}B_{13}Si_9$, $Fe_{79}B_{16}Si_5$ and $Fe_{81}B_{13.5}Si_{3.5}C_2$. The as-received specimens were cleaned with acetone before being introduced into the ultrahigh-vacuum system. All analyses were done on the shiny side, i.e. the side which was not in contact with the spinning wheel during the liquid-quenching process. The system used for the analysis was an Auger electron spectroscopy/X-ray photoelectron spectroscopy (AES/XPS) Physical Electronics Model 545 equipped with a double-pass cylindrical mirror analyser and a coaxial electron gun. The X-ray source used was a magnesium anode with exitation energy of 1253.6 eV. The base pressure of the system was better than 5×10^{-10} torr. (1 torr $= 1.333 \times 10^2$ Pa.) The XPS system was calibrated with a gold standard, using the Au $4f_{7/2}$ peak at 83.8 eV.

XPS investigations and depth profiles, using 2 keV Ar^+ ions and AES, were recorded for the as-received specimens.

For the oxidation studies, the following procedures were carried out. The specimen was first sputter cleaned until no oxygen could be detected by AES and the carbon reduced to less than 4 at %. High-purity oxygen was then introduced through a gas leak valve

and a constant partial pressure (8.3×10^{-8} torr) was maintained by a dynamic equilibrium between gas inlet and pumping rate. The pressure was monitored with an ionization gauge while the oxygen purity was checked using a mass spectrometer. All filaments except for the ion gauge were switched off during high oxygen exposures, preventing oxidation of the filaments and possible influence on the oxidation behaviour due to electron emission. After the desired oxygen exposure, the specimen was investigated by XPS and AES before the next run.

The investigations included single XPS scans of the Fe 2p, B 1s and O peaks, a complete AES spectrum and detailed AES scans for the silicon and boron peaks. The run was completed by using a multiplexer to monitor the Auger peak-to-peak heights (APPH) of the various elements during depth profiling. A defocused 2 keV Ar^+ ion gun was used for sputtering.

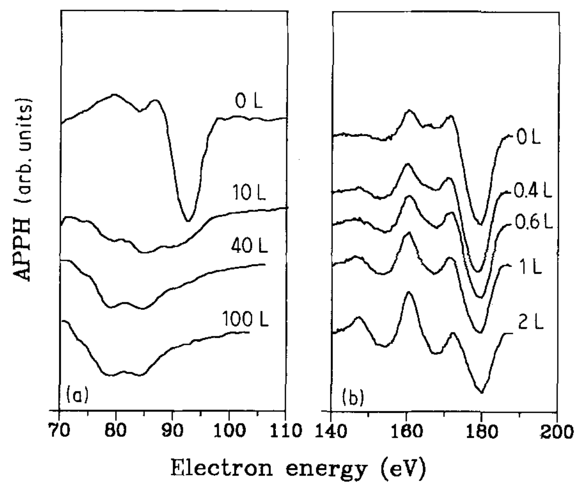

Figure 2 Development of the (a) Si 92 eV and (b) B 179 eV AES peaks as a function of oxygen exposure for the 9 at % Si alloy.

3. Results

An AES spectrum of the sputtered 5 at % Si specimen is shown in Fig. 1. Apart from the presence of chromium ($<$ 4 at %) (which was present only in the 5 at % Si specimen), some carbon contamination, even after extensive sputtering with 2 keV Ar^+ ions, can still be seen. Although the 3.5 at % Si alloy was specified to contain 2 at % C, no significant difference in the surface carbon content could be detected by AES.

Fig. 2a and b, respectively, show the change in the silicon (92 eV) and boron (179 eV) AES peaks in the 9 at % Si alloy as a result of oxygen exposure. This behaviour was observed in all three alloys investigated. Boron and silicon are elements for which AES can easily distinguish between the pure element and the oxide [8–10]. The boron-satellite peak at 168 eV, was thus used to monitor the boron-oxide APPH in depth profiling. The presence of the Fe 85 eV AES peak made it difficult to quantify the silicon oxidation by AES.

The ratio between the XPS peak heights of boron oxide and boron as a function of oxygen exposure is presented in Fig. 3. The curves are best fits through the respective data points. In this Figure one can see that

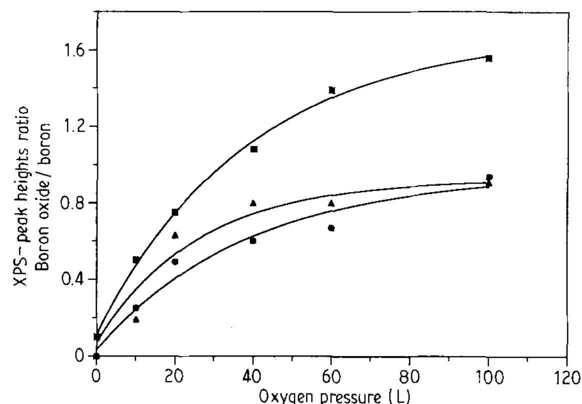

Figure 3 Ratio of the XPS peak heights of boron oxide (191 eV) and boron (187 eV) as a function of oxygen exposure. (■) 5 at %, (▲) 3.5 at % and (●) 9 at% Si alloys. Best fits through these points are represented by solid lines.

the rate of boron oxidation in the 5 at % Si alloy is consistently higher than in the other two alloys. At 100 L exposure the difference is almost a factor of two.

The chemical shift in binding energy for the Fe 2p XPS envelopes as a function of oxygen exposure for the 3.5, 5 and 9 at % Si specimens are shown in Fig. 4a–c. Included in these figures are the Fe 2p peaks for the native oxides. For purposes of comparison a plot of the iron peaks of pure iron is shown in Fig. 4d. A lower oxidation rate for iron in the amorphous alloys than for pure iron is evident. The unoxidized Fe $2p_{3/2}$ peak was situated at 706.5 eV while the *in situ* oxidation resulted in a second peak, shifted to higher binding energy at 709.5 eV. This result was found for pure iron as well as for the three amorphous alloys. For the native oxides another peak at 710.5 eV could be distinguished, indicating an additional chemical state for iron.

Fig. 5 is a typical depth profile of a 5 at % Si specimen after an oxygen exposure of 1000 L. In this Figure the APPHs of the various elements versus sputtering time is presented. Similar profiles were found for all three alloys. The figure shows a well defined boron oxide layer and a depletion of iron.

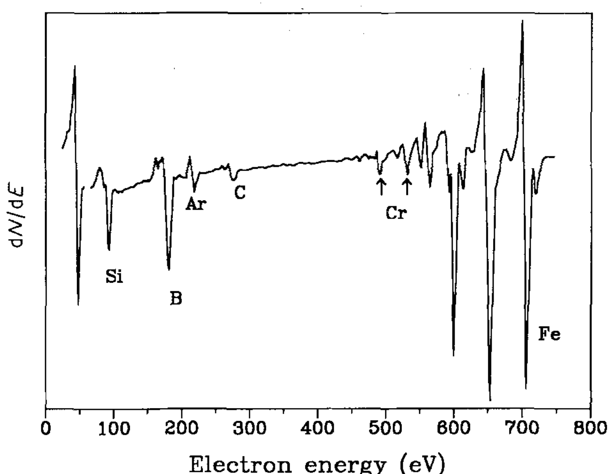

Figure 1 AES spectrum for the 5 at % Si alloy showing the presence of chromium and carbon.

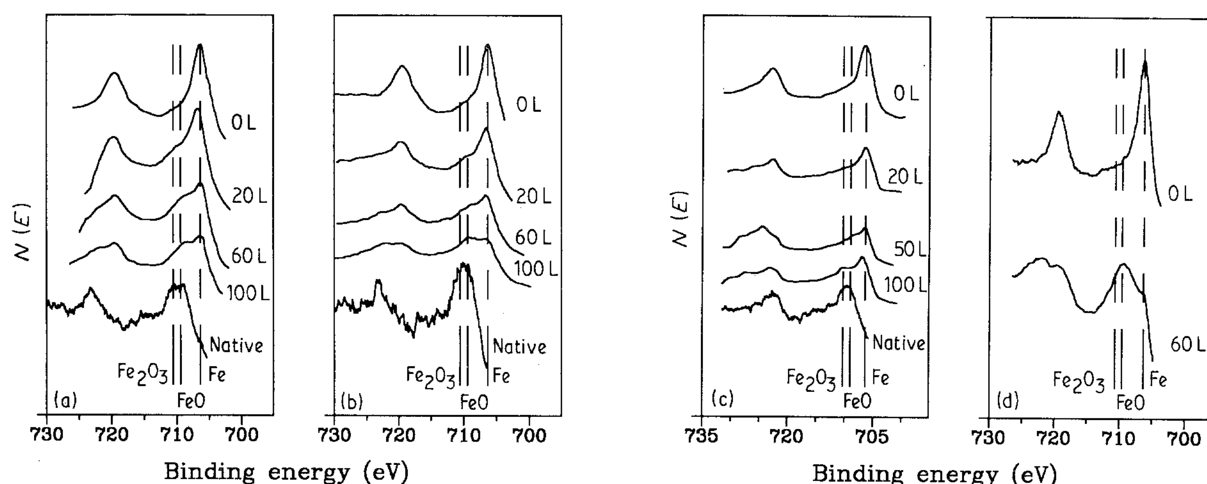

Figure 4 Development of the Fe 2p XPS peaks for the (a) 3.5 at %, (b) 5 at % and (c) 9 at % Si alloys. Included in these figures are the XPS peaks for the as-received samples. The Fe 2p envelope for pure iron is shown in (d) for comparison.

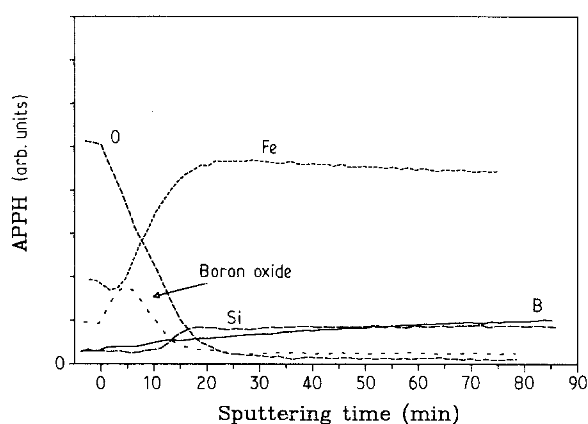

Figure 5 Depth profile for the 5 at % Si alloy after an oxygen exposure of 1000 L. The APPHs of iron, oxygen, boron, silicon and boron oxide (168 eV) are shown as a function of sputtering time. A well defined boron oxide region can be seen.

The depletion of boron between the oxide layer and the bulk is an indication of boron segregation. At the oxide–bulk interface a slight enrichment in pure silicon occurred. Similar profiles were recorded for the as-received oxides. This result indicated that the boron enrichment in the oxide layers were not sputter induced.

4. Discussion

The results will now be discussed with relation to the characterization of the oxides formed, the influence of composition on the oxidation rates and the depth profiles of the oxide layers.

4.1. Characterization of the oxides

In the detailed AES spectra of the Si 92 eV peak it was clear that silicon started to oxidize at very low coverages and saturated at about 40 L. As already mentioned, the Fe 85 eV AES peak made it almost impossible to quantify silicon oxidation without deconvolution techniques. Although silicon oxidized at an early stage, the silicon oxide could still be detected at oxygen coverages of 100 L, which indicated that the outermost layer consists of silicon. According to the shift to 78 eV of the AES transition the oxide which formed was SiO_2 [10]. Such a behaviour was also reported by Wei and Cantor [11]. They studied the oxidation behaviour of $Fe_{78}Si_9B_{13}$, one of the alloys used in this study. The techniques used were scanning and transmission electron microscopy. The oxide layers were formed by annealing the samples in air in the temperature range 300–500 °C for 1–1000 h. The segregation of silicon in that temperature range makes it perhaps difficult to compare their results directly with this work. Lee *et al.* [10] studied the initial oxidation of a polycrystalline Fe–8.75 at % Si by using AES, XPS and electron energy loss spectroscopy (EELS). They observed that a very thin SiO_2-rich external layer was formed and established preferentially at the first stage of oxidation.

In the detail XPS scans of the B 1s peaks the shifting of the B 187 eV binding energy to a higher energy of 191 eV could be clearly monitored. This shift in binding energy is more like an Fe–B suboxide than a B_2O_3 [18]. This same behaviour was reported by Nagarkar *et al.* [14]. The onset of boron oxidation at very low oxygen exposures is evident in Fig. 2b. It seems thus that there is a competition between boron and silicon at very early stages of oxidation, a suggestion also made by Karve *et al.* [12].

The iron oxidation started at about 20 L oxygen exposure (Fig. 4). The shift in binding energy from 706.5 eV for iron metal [17] to 709.5 eV for oxidized Fe $2p_{3/2}$ point to FeO that formed in the initial stage of the *in situ* oxidation [14]. For the as-received samples, two Fe $2p_{3/2}$ peaks at 709.5 and 710.5 eV could be distinguished indicating the presence of FeO and the more stable Fe_2O_3 and Fe_3O_4. According to Fig. 4, the oxidation rates in the amorphous alloys are less than for pure iron.

4.2. Influence of composition

Myhra *et al.* [2] pointed out that the presence of carbon affects the corrosion resistance of Fe–B based

alloys. They found that carbon, even present as an unintended contaminant lowered the reactivity of the surface towards oxygen by about a factor of 10 in Fe–B–Cr amorphous alloys. The surface carbon concentration in all three alloys investigated in our work was about the same and of the order of 4 at % even after extensive argon ion sputtering; see Fig. 1, where carbon is still present in the 5 at % Si alloy after sputtering. Because the comparison is made between these three alloys and because the carbon contamination as detected by AES was about the same, the influence, if any, would be the same for all three alloys. It is of interest to note that carbon was present at the surface and at the oxide/bulk interface, but not in the oxide layer.

Fig. 3 shows clearly that boron oxidizes at a higher rate in the 5 at % Si alloy than in the 9 and 3.5 at % Si alloys. The difference is more significant at an exposure of 100 L. One possibility could be the difference in silicon content. In this case one would expect a different rate for boron oxidation in the 9 at% Si alloy than in the 3.5 at % alloy with the 5 at % Si in between. From Fig. 3 the picture is very much different in that the rate is highest in the 5 at % Si alloy and lowest in the 9 and 3.5 at % Si alloys. From this observation one can deduce that the amount of silicon has no major effect on the difference in oxidation rates of boron and iron. The very small difference detected between the 9 and 3.5 at % alloys may not be experimentally significant.

As mentioned in the previous paragraph the difference in behaviour of the oxide growth due to the presence of carbon can be ignored. The oxidation behaviour of the 5 at % alloy (Fig. 3) can thus only be ascribed to the presence of chromium in the alloy. An explanation for the role of chromium in the oxidation process is not obvious, but it is of interest to note that similar effects were reported in the literature. In the case of silicon and chromium, it was found [19] that the oxidation rate of silicon in $CrSi_2$ was considerably higher than for pure silicon, with no chromium oxide being detected. Myhra *et al.* [2] found that the presence of chromium in $Fe_{70}Cr_{15}B_{15}$ promoted the initial reactivity towards oxygen by two orders of magnitude compared to $Fe_{85}B_{15}$. As far as this study is concerned, the presence of chromium affected the oxidation rate of boron. No chromium oxide or an increase in the silicon oxidation rate could be detected.

4.3. Depth profiles

The enrichment of boron in the oxide layer was reported by many authors [3, 5, 12–16]. Karve *et al.* [12] studied the oxidation behaviour of an amorphous and crystallized alloy Fe–Si–B and found no enrichment of boron in the native oxide. It seems from their results that during depth profiling they were monitoring the 179 eV boron peak. It is therefore possible that the 168 eV boron oxide peak was not included in their scans. The enrichment of boron in the as-received oxides indicated that boron segregation was not sputtered induced. It is therefore possible that the surface oxidation constitutes a driving force for boron segregation [13].

From the results one can see that the oxidation of boron serves as the main limiting factor for iron oxidation, by being a barrier for oxygen and/or iron diffusion.

5. Conclusions

It is concluded that the silicon content in the amorphous alloys studied has no major effect on the room-temperature oxidation behaviour. However, the presence of chromium in the 5 at % Si alloy enhanced the reactivity of oxygen towards boron, without affecting the silicon or iron oxidation rates significantly. No chromium oxide was detected. In the initial stages of oxidation the oxides were identified as FeO with a possible formation of a Fe–B suboxide. The depth profiles show an enrichment of boron oxide near the surface.

Acknowledgements

The financial support of this University and the Foundation for Research and Development are gratefully acknowledged.

References

1. R. W. CAHN, *Contemp. Phys.* **1** (1980) 43.
2. S. MYHRA, J. C. RIVIÈRE and L. S. WELCH, *Appl. Surf. Sci.* **32** (1988) 156.
3. P. P. KARVE, M. G. THUBE, S. K. KULKARNI and A. S. NIGAVEKAR, *Solid State Commun.* **50** (1984) 1027.
4. J. FUSY and P. PAREJA, *J. Non-Cryst. Solids* **89** (1987) 131.
5. P. SEN, A. SRINIVASAN, M. S. HEDGE and C. N. R. RAO, *J. Mater. Sci.* **18** (1983) 173.
6. O. HUNDERI and R. BERGERSEN, *Corrosion Sci.* **22** (1982) 135.
7. J. FUSY and P. PAREJA, *J. Non-Cryst. Solids* **104** (1988) 153.
8. G. N. van WYK and W. D. ROOS, *Appl. Surf. Sci.* **26** (1986) 317.
9. L. E. DAVIS, N. C. McDONALD, P. W. PALMBERG, G. E. RIACH and R. E. WEBER (eds), "Handbook of Auger Electron Spectroscopy", 2nd Edn (Physical Electronics Division, Perkin-Elmer, Eden Prairie, MN, 1978).
10. Y. P. LEE, A. J. BEVOLO and D. W. LYNCH, *Surf. Sci.* **188** (1987) 267.
11. G. WEI and B. CANTOR, *Acta Metall.* **36** (1988) 2293.
12. P. P. KARVE, S. K. KULKARNI and A. S. NIGAVEKAR, in "Rapidly Quenched Metals", Vol. 2, edited by S. Steeb and H. Warlimont (Elsevier, B.V., 1985) p. 1477.
13. D. J. de WET and G. N. van WYK, *J. Mater. Sci.* **24** (1989) 2239.
14. P. V. NAGARKAR, S. K. KULKARNI and E. UMBACH, *Appl. Surf. Sci.* **29** (1987) 194.
15. S. MYHRA and J. C. RIVIÉRE, *J. Non-Cryst. Solids* **99** (1988) 244.
16. D. R. BAER, D. A. PETERSEN, L. R. PEDERSON and M. T. THOMAS, *J. Vac. Sci. Technol.* **20** (1982) 957.
17. D. R. HUNTLEY, S. H. OVERBURY, D. M. ZEHNER, J. D. BUDAI and W. E. BROWER, *Appl. Surf. Sci.* **27** (1986) 180.
18. G. MAVEL, J. ESCARD, P. COSTA and J. CASTING, *Surf. Sci.* **35** (1973) 109.
19. G. L. P. BERNING, *Appl. Surf. Sci.* **40** (1989) 209.

Received 7 November 1990
and accepted 10 April 1991